

Encapsulating Amidoximated Nanofibrous Aerogels within Wood Cell Tracheids for Efficient Cascading Adsorption of Uranium Ions

Weihua Zhang, Chunlin Xu, Xinpeng Che, Ting Wang, Stefan Willför, Mingjie Li,* and Chaoxu Li*



Cite This: *ACS Nano* 2022, 16, 13144–13151



Read Online

Chaoxu Li, Mingjie Li, Weihua Zhang, Xinpeng Che, Ting Wang

*Group of Biomimetic Smart Materials, Qingdao
Institute of Bioenergy and Bioprocess Technology, Chinese
Academy of Sciences & Shandong Energy Institute, Qingdao 266101, P. R.
China; Center of Material and Optoelectronics Engineering, University of
Chinese Academy of Sciences, Beijing 100049, P. R. China;*

Chunlin Xu, Stefan Willför

*Laboratory of Natural Materials Technology,
Åbo Akademi University, Turku FI-20500, Finland*

Published on-15th Aug 2022

PAPER PRESENTATION
TANMAYAA NAYAK
06.01.2023

Introduction

- Here they have adopted a filtering adsorption technique for selective uranium extraction from seawater.
- Here they preferentially exfoliated cellulose fibrils from the lignin-poor layer of secondary cell walls of balsa wood during an *in situ* amidoximation process.
- By maintaining honeycomb-like cellular microstructures and cellulose aerogel stuffing in their cell tracheids, the resultant nanowoods showed superior mechanical properties with large surface areas ($\sim 80 \text{ m}^2 \text{ g}^{-1}$).
- In analogy to a typical cascading filtration system, the filtrate passed successively the layered-organized cell tracheids through abundant micropores on their cell walls, enabling a high rejection ratio of $>99\%$ and flux of $\sim 920 \text{ L m}^{-2} \text{ h}^{-1}$ under pressure up to 6 bar (membrane thickness of 2 mm).

Why this paper?

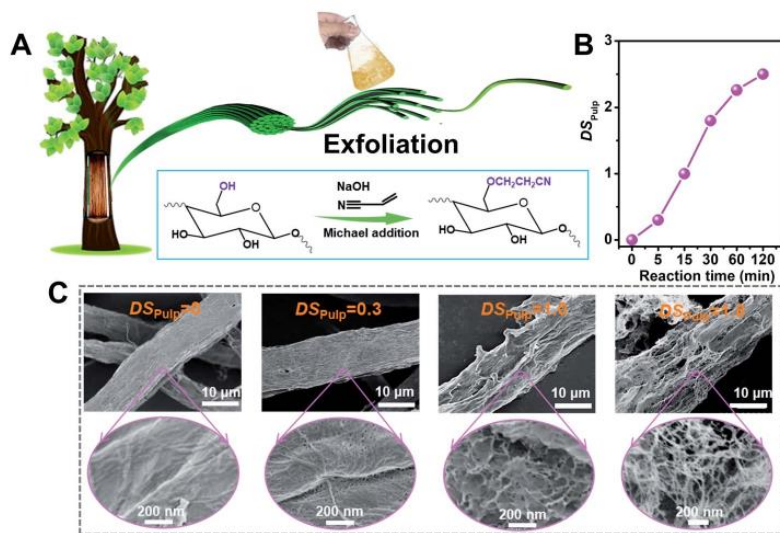
- This study provides an *in situ* approach to producing robust woods with functional nanocellulose encapsulated into their cell tracheids.
- It also offers a sustainable route for the high-efficiency extraction of aqueous uranium.



Cite this: *J. Mater. Chem. A*, 2022, 10, 7920

Rapid and manual-shaking exfoliation of amidoximated cellulose nanofibrils for a large-capacity filtration capture of uranium†

Weihua Zhang,^{ab} Xiao Han,^{bc} Jun You,^{ID d} Xiaofang Zhang,^{bc} Danfeng Pei,^{bc} Stefan Willför,^a Mingjie Li,^{*bc} Chunlin Xu ^{ID *a} and Chaoxu Li ^{ID *bc}



Pathway followed to exfoliate cyanoethylated cellulose fibrils by manual shake. (A) Cyanoethylation of the commercial softwood pulp. The top-right inset gives its SEM image after cyanoethylation. (B) Variation of cyanoethyl degrees of substitution (DS_{pulp}) with reaction time. (C) SEM images of the cellulose pulp fiber with different cyanoethylation DS values.

Uptake capacity- 1327 mg g^{-1}

Rejection ratio of $>99\%$

Flux - $48 \text{ L m}^{-2} \text{ h}^{-1}$ for a $2.5\text{-}\mu\text{m}$ -thick membrane under 0.95 bar .

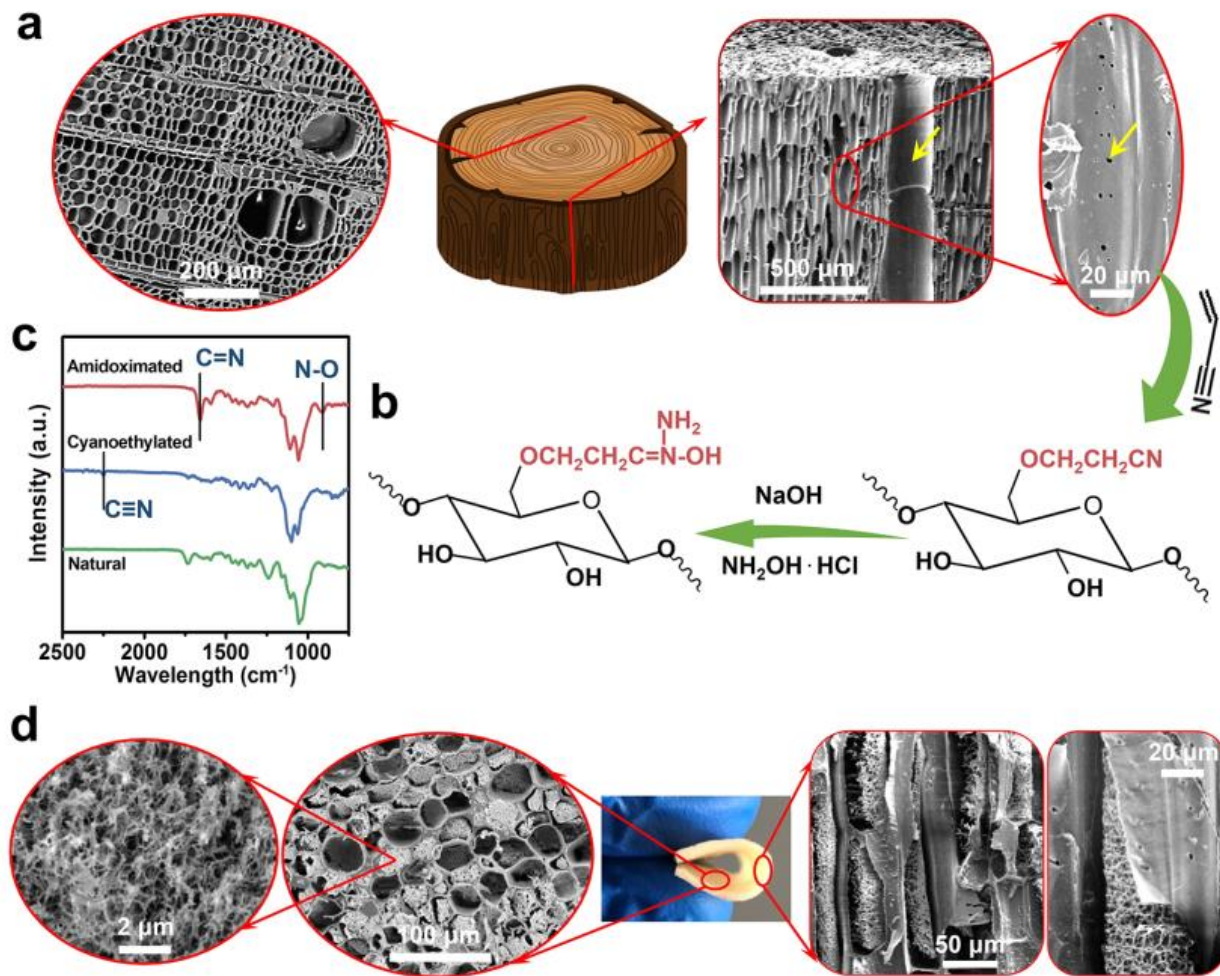


Figure 1. Pathway followed to encapsulate amidoximated cellulose fibrous aerogels within wood cell tracheids. (a) Cross-section and longitudinal view of balsa wood. Micropores on the tracheids' walls are indicated with the yellow arrow. (b) *In situ* cyanoethylation and amidoximation of cellulose in natural balsa wood. (c) FT-IR spectra of natural, cyanoethylated, and amidoximated cellulose. (d) Crosssection and longitudinal view of amidoximated wood with fibrous aerogels encapsulated in cell tracheids.

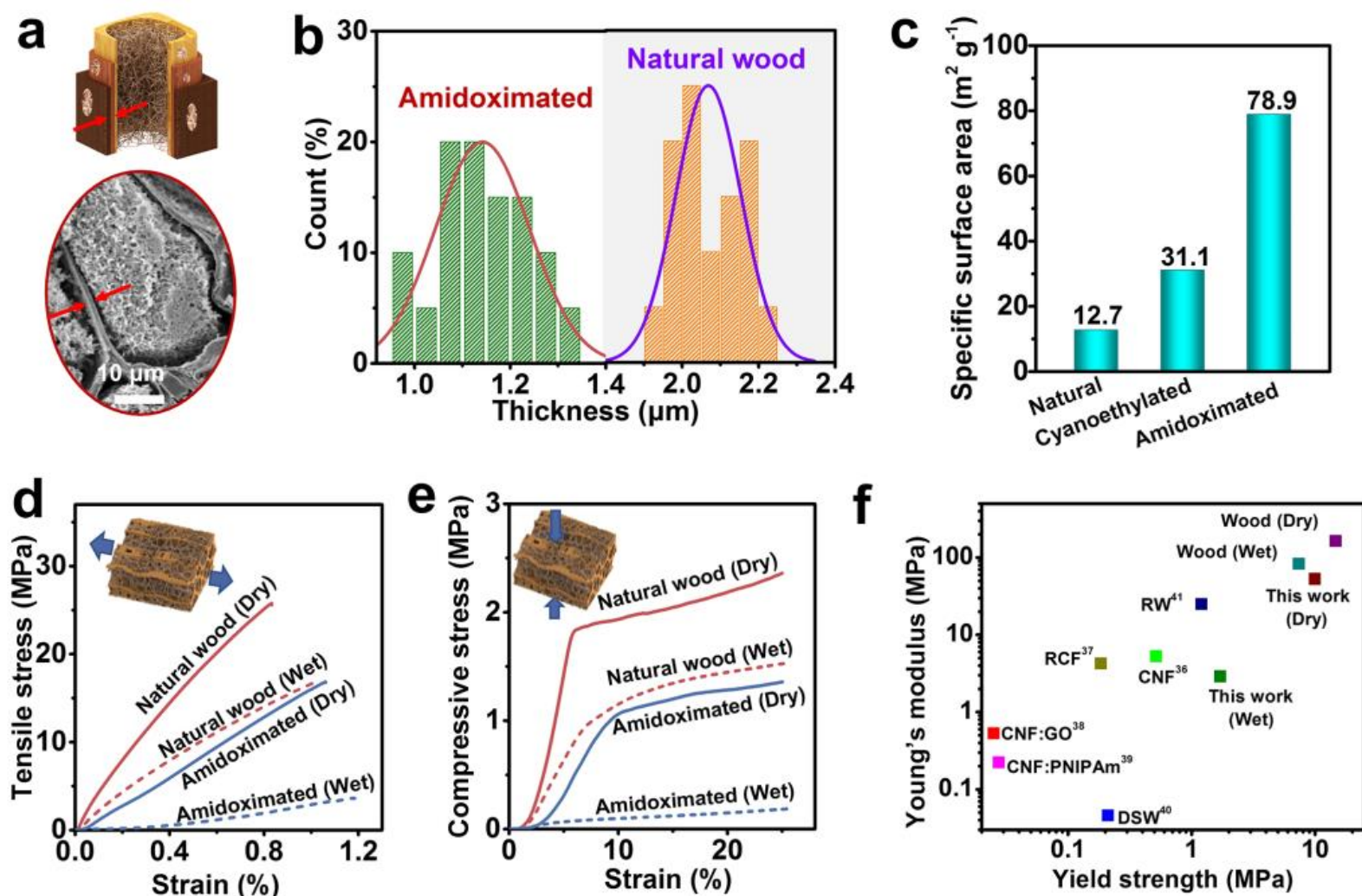


Figure 2. Physical characterization of amidoximated wood. (a) Schematic illustration and SEM image of amidoximated fibrous aerogels within a wood cell. (b) Cell wall thickness distribution of natural wood and amidoximated wood. (c) Specific surface area of natural, cyanoethylated, and amidoximated wood. (d) Comparison of tensile stress-strain curves of natural wood and amidoximated wood along the longitudinal direction at dry and wet states. (e) Comparison of compressive stress-strain curves of natural wood and amidoximated wood along the transverse direction at dry and wet states. (f) Comparison of Young's moduli and compressive yield strength of amidoximated nanowood along the longitudinal direction to those of cellulose-based aerogels and foams reported in the literature.

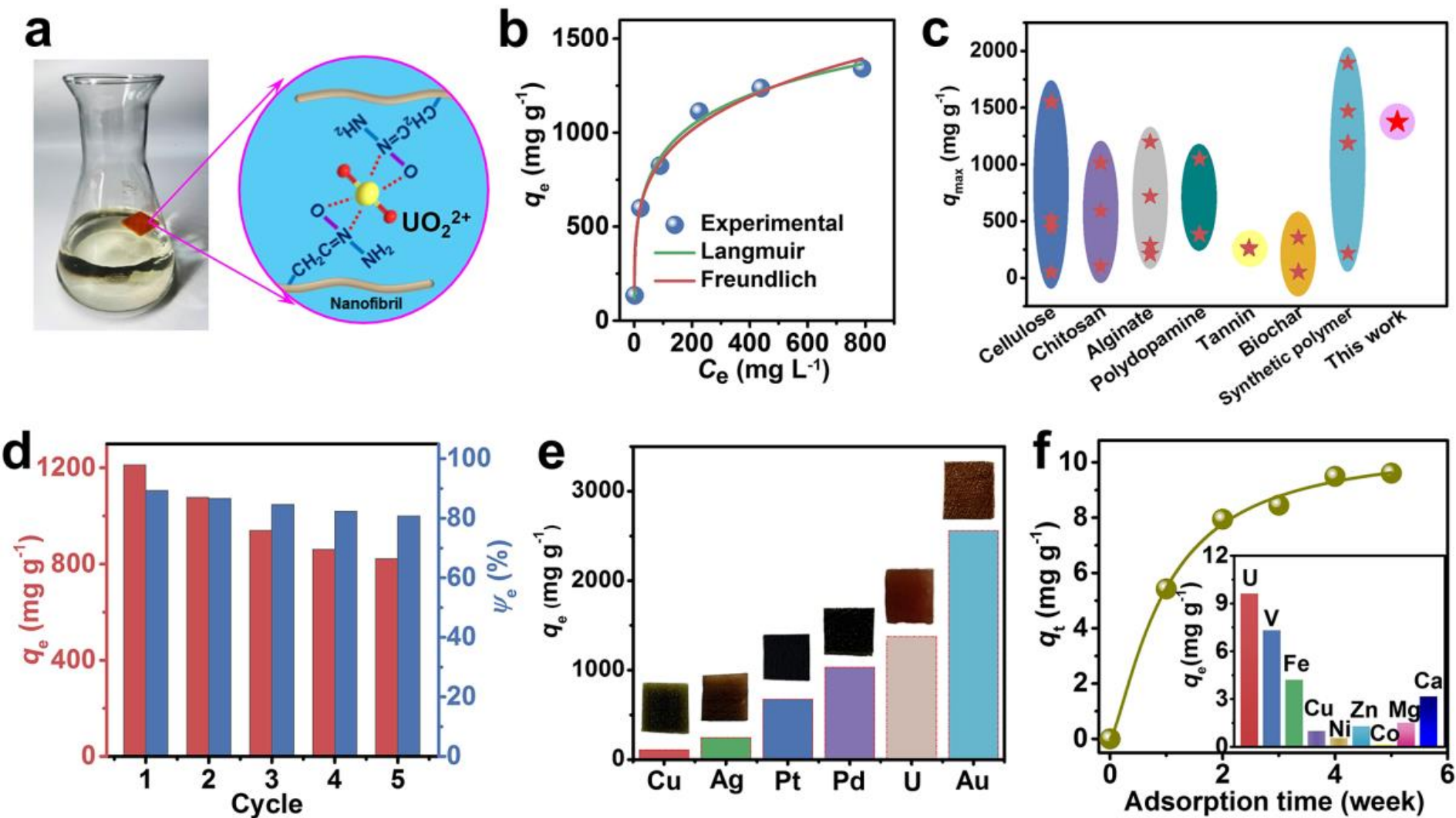


Figure 3. Static adsorption of uranium ions with amidoximated wood. (a) Schematic illustration of chelating uranyl ions with amidoxime groups. (b) Adsorption isotherm curve fitted with Langmuir and Freundlich models ($\text{pH} \approx 8$); q_e is the equilibrium adsorption capacity, and C_e is the equilibrium concentration. (c) Comparison of uranium adsorption performance to those of various polymer adsorbents (detailed in Table S4); q_{\max} is the maximum adsorption capacity. (d) Adsorption-recovery performance during the cyclic adsorption and desorption of uranium ions; Ψ_e (%) is the equilibrium elution efficiency. (e) Maximum adsorption capacities of various metal ions by amidoximated nanowood. (f) Cumulative amount of uranium ions adsorbed in natural seawater in 5 weeks; q_t is the adsorption capacity at time t . The adsorption capacities of other coexisting ions in natural seawater are shown in the inset.

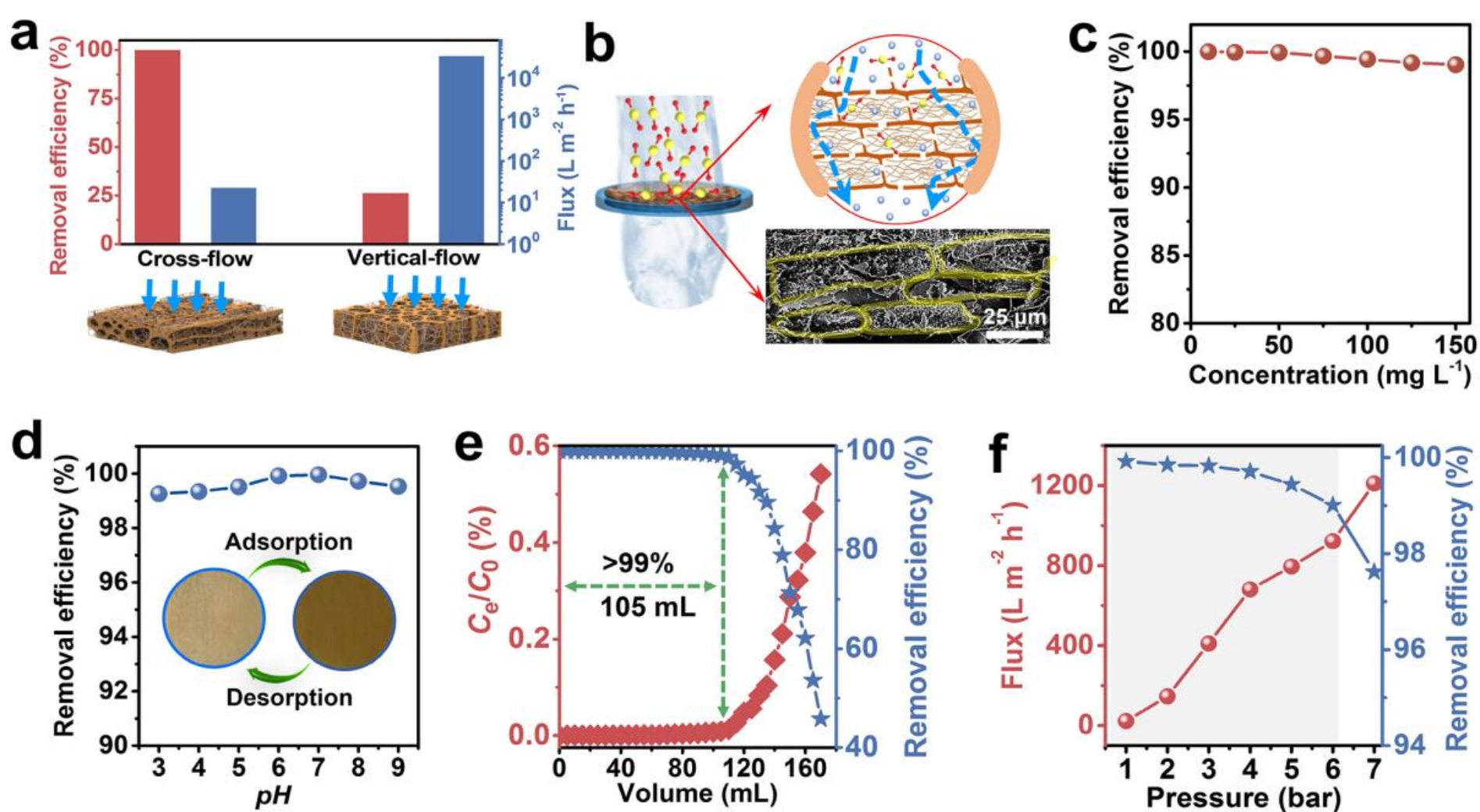


Figure 4. Cascading filtration of aquatic uranium ions with amidoximated wood. (a) Comparison of removal efficiency and flux, indicated as cross-flow and vertical-flow. (b) Schematic illustration of cascading filtration across layered-organized cell tracheids. A thermoset polymer was used to seal the membrane edge to avoid the possible side leakage. The cell tracheids were interconnected by the micropores on their walls. (c) Effect of uranium concentration on removal efficiency. (d) Effect of pH on uranium removal efficiency. Initial uranium concentration: 25 mg L^{-1} . The inset shows the amidoximated wood after adsorption and desorption. (e) Variation of filtrate concentration and removal efficiency with the volume of the filtering solution. (f) Permeation flux and removal efficiency under different pressures. The initial uranium concentration was 50 mg L^{-1} and the membrane thickness was $\sim 2 \text{ mm}$; $\text{pH} \approx 8$.

Conclusion

- The resultant wood presented a large specific surface area ($\sim 80 \text{ m}^2 \text{ g}^{-1}$) and excellent mechanical properties.
- A maximum U(VI) adsorption capacity of 1375 mg g^{-1} was achieved in simulated seawater.
- This study not only provides an efficient and *in situ* approach to producing robust nanowoods with functional nanocellulose encapsulated into the cell tracheids but also promises a green and high-efficiency route for cascading adsorption filtration of aquatic uranium ions.

Thank you